Liquid Metal Flow Studied by Positron Emission Tracking

Dybalska, Agnieszka; Caden, Adrian J.; Parker, David J.; Wedderburn, John; Griffiths, William D.

DOI:
10.1007/s11663-020-01897-7

Document Version
Publisher's PDF, also known as Version of record

Citation for published version (Harvard):
Dybalska, A, Caden, AJ, Parker, DJ, Wedderburn, J & Griffiths, WD 2020, 'Liquid Metal Flow Studied by Positron Emission Tracking', *Metallurgical and Materials Transactions B*, vol. 51, no. 5, pp. 1912-1917. https://doi.org/10.1007/s11663-020-01897-7

TOPICAL COLLECTION: LIQUID METAL PROCESSING & CASTING CONFERENCE 2019

Liquid Metal Flow Studied by Positron Emission Tracking

AGNIESZKA DYBALSKA, ADRIAN J. CADEN, DAVID J. PARKER, JOHN WEDDERBURN, and WILLIAM D. GRIFFITHS

To improve the properties of castings, a new technique to observe the fluid flow and study the motion of oxygen-bearing inclusions has been developed. This new technique, Positron Emission Particle Tracking (PEPT), enabled a single radioactive tracer particle, moving inside a liquid metal casting, to be tracked with an accuracy of some millimeters, depending on the properties of the liquid metal and the mold. These novel experiments give promising results to observe the liquid metal flow and locate the tracked particle in a casting. Experiments have shown that various particle sizes (200 to 600 μm presented here) can be used to observe the liquid metal flow, if the particle has sufficiently initial radioactivity. Different sizes of particles are considered and their radioactivity compared in terms of their usefulness for tracking in flowing liquid aluminum according to the specific surface area.

https://doi.org/10.1007/s11663-020-01897-7

I. INTRODUCTION

INCLUSIONS in castings are well known for their harmful role. Indigenous inclusions, which originate from the liquid metal, are almost impossible to avoid. For example, oxidation occurs naturally when liquid metal is in contact with the oxygen present in the atmosphere.[1–4] Such an oxide film can be entrained into the melt by surface turbulence and folded into bifilm defects of different sizes and shapes. These inclusions can cause major reductions in the strength or fatigue resistance of castings.[5] Oxide films lead to additional problems such as decreased fluidity and feeding,[6] creation of leakage paths due to connecting wall-to-wall defects in castings[5] and reduced machinability.[7,8] The means to eliminate such defects is limited, (although it has been suggested that with sufficient control on the oxide phase formation an improvement in the final properties of the Al alloy may be obtained.[9] One way to eradicate such defects may be the possibility to observe inclusion behavior during casting. In recent years, a new technique to observe fluid flow and study the motion of oxygen-bearing inclusions has been proposed. This new technique, Positron Emission Particle Tracking (PEPT), enables a single radioactive tracer particle moving inside a liquid metal casting to be tracked with an accuracy of some millimeters, depending on the liquid metal and mold properties. PEPT, developed at the University of Birmingham, is a variant of the standard imaging technique used to determine the spatial distribution of a fluid tracer, a technique known as Positron Emission Tomography (PET). PEPT does not require detection of a very large number of γ-ray pairs, as does PET, which makes it a relatively fast technique, useful in a wide range of applications. Both methods rely on the detection of radioactive particles containing an isotope which decays by positron emission. Emitted positrons collide with local electrons and annihilate causing the emission of γ-rays which can be detected externally from an otherwise opaque media. More details of the PEPT technique and its uses can be found elsewhere.[10–16] The PEPT experiments have been compared with CFD simulations[17,18] and other commonly used visualization techniques, such as Particle Image Velocimetry (PIV)[19] with good agreement being obtained. Previous studies carried out on the application of this technique for opaque liquid, which included tracking of radioactive particles in steel castings,[20] and Al alloy sand castings[21] showed promising results to observe liquid metal flow and locate tracked particles in cast metals. The inclusions present in the casting are mostly oxides and the benefit of this technique is that commonly used tracers, such as oxides such as alumina, are also those

AGNIESZKA DYBALSKA, ADRIAN J. CADEN, DAVID J. PARKER, JOHN WEDDERBURN, and WILLIAM D. GRIFFITHS are with the School of Metallurgy and Materials, University of Birmingham, B15 2TT, Birmingham, UK. Contact e-mail: A.Dybalska@bham.ac.uk
Manuscript submitted December 23, 2019.

Published online: 06 July 2020

compounds that occur naturally in liquid metal. To improve the technology, there have been several attempts to prepare smaller tracers, of a size comparable with the dimensions of typically occurring natural inclusions. Except for a few experiments, there have been no reproducible methods to prepare tracer particles smaller than 200 μm. The particles used as tracers need to have sufficient initial radioactivity to be detectable within the lifetime of an experiment, governed by the half-life of the radioactivity of the tracer particle used.

Direct labeling used commonly is giving the oxides particles activity levels 4 times smaller than indirect labeling developed at the University of Birmingham.[22] This paper describes the comparison of differently labeled particles in the context of their usability as tracking particles in liquid Al alloy castings.

II. EXPERIMENTAL PROCEDURE

The 3 ml water necessary to prepare tracers was made radioactive by bombardment in a 33 MeV 3 He beam. The oxygen present in the water was partially converted into radioactive fluorine-18. About 1 ml of the prepared radioactive water was poured into a glass container within which were an amount of tracer particles. The water in the container was evaporated in a stream of nitrogen and an infrared lamp. The particles used as tracers are usually oxides, but in this work HA (hydroxyapatite) particles were used as well. The exact mechanism of attachment of radioactive fluorine-18 to the surface of an alumina particle is not yet known but may be caused by surface adsorption forces.[22] The particles used had sizes of between 40 and 600 μm. The nominal sizes of the powders are given as described by the suppliers. Usually, the different powders were present in sizes of about 5 to 10 pct of their nominal size. The measurements of surface area were made by a 3 Flex Surface Characterization Analyzer from Micromeritics Instrument Corporation. The surface area was determined by the Brunauer–Emmett–Teller (BET) model by nitrogen adsorption, measured as a function of relative pressure.[23] A scanning electron microscope (SEM) was used to observe the surface of the particles to be tracked, using a JEOL–JSM-6060 instrument with nominal resolution of 3.5 nm at 30 kV. A PROTO AXRD Benchtop powder diffraction system was used for XRD (X-ray diffraction) analysis. To perform the tracking experiments the liquid aluminum was poured into specially prepared sand molds. During the casting experiments, the PEPT detectors were positioned in a square pattern around a resin-bonded sand mold set diagonally within this square. The mold cavity of the castings used in the experiments consisted of plates of sizes 200 mm $\times$ 100 mm and 15 mm in depth, filled by a running system providing a bottom-filled approach. Near the top of the downsprue, a hole through the mold was prepared to hold a 3 mm metal rod containing a radioactive particle. To keep the particle inside the metal rod, a blind hole with a diameter of 1 mm and 5 mm in depth was crimped closed at around 2 mm from the open end (see Figure 1). When the mold was placed inside the array of detectors a radioactive tracer particle was positioned at several reference points, which was later used to correct alignment errors between the mold and the coordinate system when plotting particle tracks. The sand molds were cast with liquid commercial purity aluminum alloy at about 760 °C, whereupon the liquid metal was released into the downsprue, causing the 3 mm aluminum rod to melt, releasing the radioactive particle into the metal stream. Since the cast plate was only 15 mm thick, and the positron camera had a resolution of 4 to 8 mm in each axis, only plan views of the particle tracks within the castings were determined.

III. RESULTS AND DISCUSSION

A. *Casting Experiments*

Figure 2 shows recorded tracks of the radioactively labeled particles collected during the casting experiments. The particle traveled with the liquid metal as it flowed down the downsprue, along the running system and into the mold cavity. The initial and final positions of the particles were marked on the graphs as bright points, since these were the points where the particle was stationary for a period of time. The initial position was, of course, outside the mold cavity casting plate which led to some error in the positioning of the detectors. The final particle position was believed to be located, with a maximum error of about 5 to 7 mm, in the mold cavity.[24–26]

The results were deemed to be highly reproducible, except in one case when the particle became lodged inside the downsprue. The final position of the particles was usually close to the top of the mold, which may have been influenced by the small air bubble trapped inside the introduction rod containing the radioactive particle. (The next step could develop the introduction technique to avoid the presence of the air bubble, *e.g.*, by filling the hole with Al powder). From the recorded movement, it

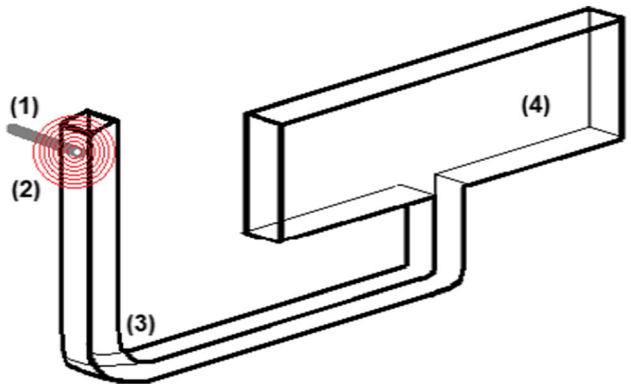

Fig. 1—Casting experiment setup: the aluminum rod (1) containing the radioactive particle (2) was placed through the mold into the downsprue, and was melted when the mold cavity was filled through the downsprue (3) carrying the radioactive particle along the running system and into the mold cavity (4).

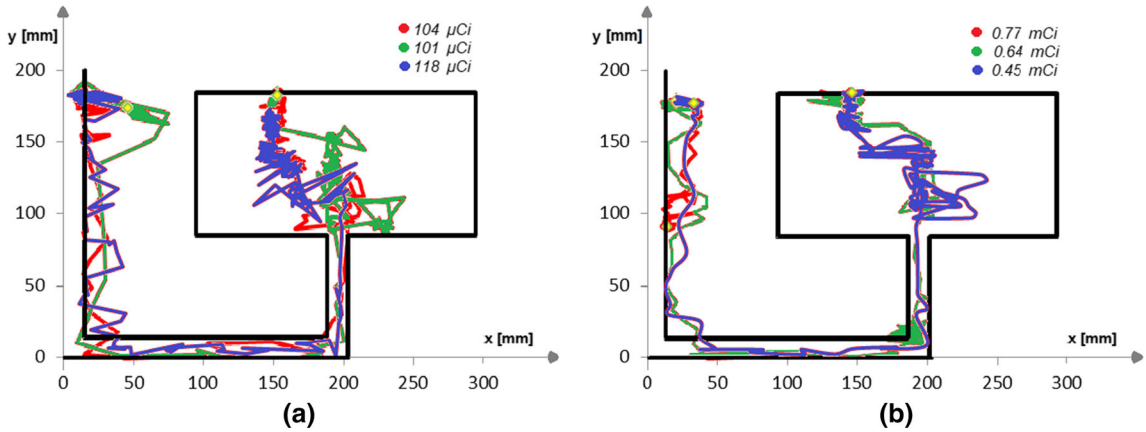

Fig. 2—Tracks of radioactive particles in the liquid aluminum flow, cast at about 760 °C; (*a*) 200 μm and (*b*) 600 μm alumina particles. The activities stated were those calculated at the beginning of the filling of the mold.

can be seen that smaller particles gave more complicated tracks, implying that the tracking process in that case was more accurate. The question is, what is the influence of the air bubble trapped in the Al rod upon insertion in the liquid metal. More complicated tracks were associated with 200 μm particles (see Figure 2), possibly because in this case the air bubble would be expected to be larger, we can assume that the attached bubble did not prevent the free movement of that particle. Thus, the particle movement can be treated as representing the track of the inclusion created at the beginning of the process of filling the mold. Since the setup is the same each time, similar behavior of the particle track would be expected. The tracks observed were similar but not identical, (compare the track the first and second particle in Figure 2(b)), which shows the potential sensitivity of the technique. In the future, the technique is intended to be used for tracking the behavior of inclusions in more complicated cases. However, the process still needs to be optimized, and more useful results may be expected with smaller tracers. Considering that the typical inclusion sizes found in liquid metals are believed to have sizes of about 0.2 to 30 μm for aluminium, or starting from 10 μm for magnesium oxide and spinel,[5] the tracers should be smaller than previously used (110 to 600 μm).[25,26] To find the best tracers one has to take into account the attenuation present in the system and compare it with the initial radioactivity of tracers. Gamma radiation is absorbed by the materials between the particle and the detectors. Firstly, the radiation will travel inside the aluminum casting, then through the sand walls of the mold and finally will be detected by the detectors. The path of the radiation in the materials will be shortest when the γ-ray travels perpendicular to the mold walls and will be longest if the angle between γ-rays and the wall will be 45 degrees. Thus, following the attenuation calculations presented before for this setup[25] based on Lambert's law, the range of attenuation will be between 84 and 86 pct. After a number of experiments, it was estimated that the approximate level of radioactivity possible to be detected by the detectors is about 7 μCi.[25] This value is calculated to be the effective radioactivity after attenuation at the time of use, which can be detected taking into account the scattering and inaccuracy of the system.

IV. PARTICLE LABELING

The preparation of the casting experiments requires about 200 minutes in time. During this time the particles are embedded in the radioactive water, dried, separated by a needle under a microscope, measured and transported to the site of the casting. Similarly, the preparations for casting require melting of the alloy and mounting of the radioactive rod in the correct position within the mold. This time can be shortened if necessary but is an optimum time used in the present conditions. To detect 7 μCi of radioactivity, the particle should have radioactivity of over 50 μCi at the moment of use. Thus, any alumina particle, which after 200 minutes will still have activity 50 μCi, can be used in the experiments.

Furthermore, using the radioactive decay of Fluorine-18, it can be calculated that the initial radioactivity of the particle needs to be about 180 μCi.

In Table I, the measured activities of different particles used in this work are compared.

Based on the data presented here, the radioactivity of the particles will be dependent on their surface area. Particles with sizes of about 350 μm were reported to be less radioactive after indirect labeling, as described in the experimental procedure. The particles were determined by XRD to be α-alumina (see Figure 3,[27]). Table I shows significant differences in the surface area for different sizes of alumina, (reported previously[28]), which agreed well with measurements reported here (0.4 m^2/g for alpha-alumina, reported in reference,[28] when the powder was prepared by strong heating). Even though some attempts to prepare the alpha-alumina with a higher surface area have been made,[28] γ-alumina is still commonly used as a catalyst because of the possibility to prepare the high surface area to increase the catalytic reactivity.[29] As mentioned before in the experimental procedure, the mechanism of indirect radioactive labeling is believed to be associated with

Table I. Activities Measured and Calculated After 200 min for Different Types of Alumina Particles. The Phase Was Confirmed by XRD Analysis

Particle Size [μm]	Phase	Surface Area [m^2/g]	Water Activity Used [mCi]	Processing Time	No. of Particles Used	Average Activity Per Particle (Measured) [μCi]	Average Activity Per Particle After 200 Min [μCi]	Relative Particle Activity[#]
600	γ	175±12	11.6	70 min	5	1360	600	18.2 pct
350	α	0.42±0.01	Reported as not sufficiently active to perform tracking experiments					
180 to 210	γ	84±5	9.4	80 min	5	1270	595	23 pct
90 to 125	γ	125±6	13	60 min	5	124	51	1.4 pct
100	γ	146±7	13.8	100 min	10	154	82	2.2 pct

[#]Compared with the radioactivity of the water—the ability of the particle to bond with the radioactive ions present in the water.

greater radioactivity, caused by ion adsorption to the particle surface.[22] Thus, the surface area may play an important role in the preparation of radioactive tracers, especially when individual particles are considered.

One can compare two similarly sized powders from Table I, a powder of size 90 to 125 μm with a smaller surface area (125 m^2g^{-1}) and a powder with a nominal size of 100 μm, (146 m^2g^{-1}). The radioactivity of the average single particle was larger for the 100 μm powder than for the particle of 90 to 125 μm size, regardless of its slightly smaller size. It is reasonable to compare the ability to pick up the radioactivity from the water and Fluorine-18 solution. For 100 μm particles the final activity was about 2.2 pct of the used water activity. Particles with a size range of 90 to 125 μm were able to pick up only about 1.4 pct of the applied radioactivity, giving an average value of the radioactivity of about 50 μCi, placing that powder exactly on the border of usability in the liquid metal experiments described here.

The mean values of the particle radioactivities provide an overview of the efficiency of the labeling process for different powders. Unfortunately, this information did not explain all observations, especially the quite large scattering in the radioactivity of single particles. The observed radioactivity differed from 40 μCi to 1270 μCi for particles separated from the powder with a nominal size of 200 μm. To explain this the SEM pictures of both particles were analyzed to find any differences in the structure of both particles.

Comparing both particles a size difference was observed. The first particle had a diameter of 190 μm, the second about 216 μm, (these values were the mean of 10 measurements). According to measured diameters, the surface area of the sphere was calculated. The difference is only about 30 pct and does not explain why the radioactivity of the smaller particle was 30 times higher. The SEM images showed that the more radioactive particle had a much less uniform surface than the particle with smaller radioactivity. The corrugated surface of the more active particle could be the reason why more radioactive ions present in the water joined to this particle surface than to the other one. The SEM images can be treated as indirect evidence that the surface area is one of the most important factors which should be considered in making an individual tracer with sufficient activity to be easily tracked.

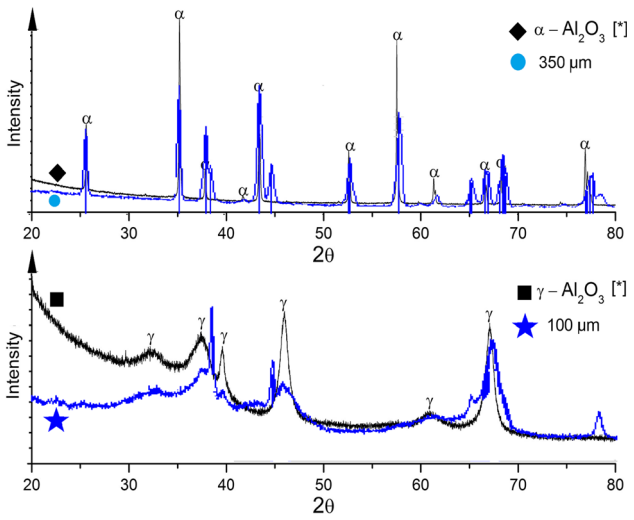

Fig. 3—XRD spectra recorded for particles of 350 μm size (reported as not active during several experiments) and for 100 μm powder. Both spectra are overlaid on known alpha and γ-alumina XRD spectra [*] with specific peaks marked.[27]

To consider other types of powders as potential tracers for the liquid metal experiments, the radioactivity of 50 mg of each powder was measured and compared with the powders presented earlier. The results are given in Table II.

To find a potent tracer, two different types of powders were compared. First, previously analyzed γ-alumina powders of different sizes were activated. Secondly, hydroxyapatite particles of two different sizes were considered. The reason for using the hydroxyapatite was its relatively high melting temperature (1100 °C) and reported usability as a potent tracer.[25] We plan to use hydroxyapatite for future experiments. In terms of the number of particles (50 mg), the activities were not so widely scattered. Much greater differences when the radioactivity of individual particles was measured. The bulk powder (50 mg) activity measurements gave some idea about which powder can be considered for individual particle activation. One fact which can be considered is that the surface area of the powder may not significantly influence the measured radioactivity for the bulk powder. Table III shows the radioactivity of 0.05 g γ alumina particles with similar particle sizes—40

Table II. Radioactivity of 50 mg of Different Powders Calculated at the Same Time After Direct Measurements. The Same Initial Activity of Water Was Used

Particle Size	Material	Surface Area [m^2/g]	Radioactivity [mCi]
600 μm	alumina	175±12	3.06
90 to 125 μm	alumina	125±6	2.96
100 μm	alumina	146±7	2.82
50 μm	alumina	191±13	2.84
50 to 80 μm	HA	—	2.19
< 200 nm	HA	—	2.81

Table III. Radioactivity of Powders with Relatively Similar Sizes and Different Surface Area

Particle Size [μm]	Surface Area [m^2/g]	Particles Amount [g]	Measured Activity of Used Amount [mCi]
50	191±13	0.05	1.98
40	105±6	0.05	1.88

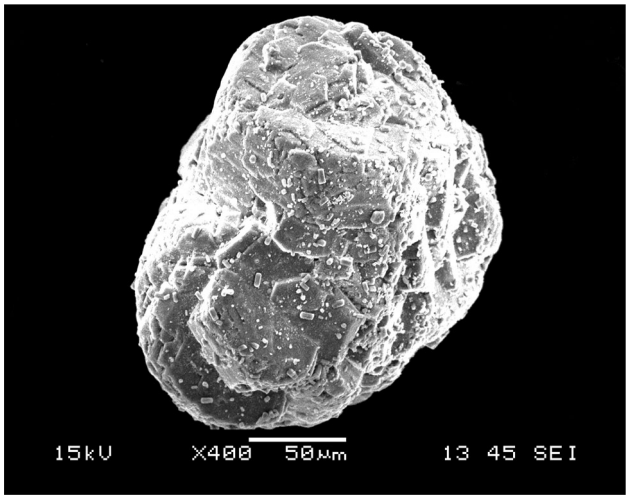

Fig. 4—Particle 1 (from 200 μm nominal size powder)—activity 40 μCi.

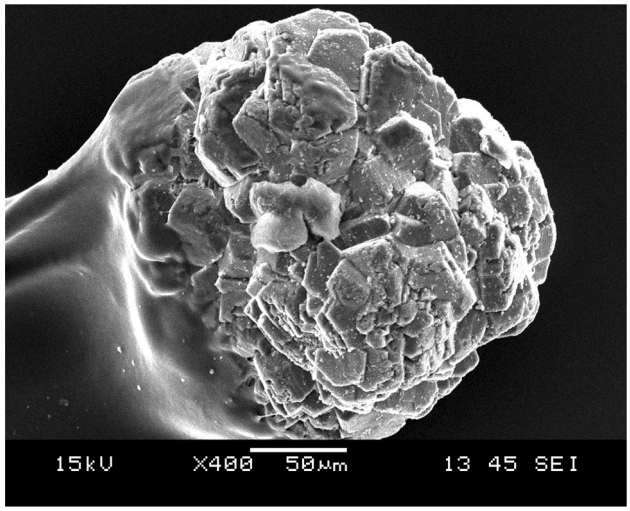

Fig. 5—Particle 2 (from 200 μm nominal size powder)—activity 1270 μCi.

and 50 μm. The surface area of the 50 μm powder was almost double in size the surface area measured for the 40 μm powder. The measured activity difference was small (about 5 pct). Still, the radioactivity of individual separate particles may be significantly different, as seen for the 200 μm particles (see Figures 4 and 5).

From Table II, hydroxyapatite seemed to be less potent than alumina in terms of radioactivity determined after labeling. The initial activity of the water was the same for all powders and their activity was calculated at the same time. In that way, all activities presented in Table II can be compared. Interestingly, the alumina particles having a quite small size, (about 50 μm), were well activated, giving a similar amount of radioactivity as determined before with 100 μm particles, which had mean particle radioactivity of 82 μCi, (predicted at the time of use). The surface area of 50 μm alumina seemed to be large (190 m^2/g), almost twice that measured for the alumina powder of size 90 to 125 μm. (The 90 to 125 μm alumina exhibited particle radioactivity that was just on the border of being detectable). This suggests that 50 μm particles could be used as tracers in liquid metal experiments. Unfortunately, physical handling of particles smaller than about 100 μm is very difficult, having health and safety implications. Direct measurements of individual particle activities still require more experimental work.

As seen in the case of particles presented in Figures 4 and 5 some correlation of the surface area with the activity of the individual particles is likely. Unfortunately, the measurements of the surface area for the individual particles were extremely difficult. The activities presented in Table III were measured for a large number of particles. As has been seen, the activity of

each tracer particle can be very scattered, so the next step will focus on the measurement of the activity of individual particles from the alumina powder, with a nominal size of 50 μm. From these results, this powder seems most useful in experiments with liquid Al.

V. SUMMARY

The PEPT technique has given promising results in the liquid metals, offering a new tool to track the behavior of inclusions in liquid metals. To model this behavior more closely, an attempt to find optimal tracking particles has been made. The most promising medium is γ-alumina powder, which was found to be most potent in terms of bonding with radioactive ions. The radioactivity achieved was measured for specific particles and specific amounts of powders (50 mg). These measurements suggest that 50 μm γ-alumina particles in the liquid metal experiments are most useful, because the particles possess a relatively high surface area. Further experiments in liquid metal are planned to verify those findings.

ACKNOWLEDGMENTS

The authors acknowledge financial support from the ExoMet Project (co-funded by the European Commission contract FP7-NMP3-LA-2012-28042) and the UK Engineering and Physical Sciences Research Council (EPSRC) through grants EP/P034411/1, EP/R000239/1 and EP/R002037/1.

OPEN ACCESS

REFERENCES

1. W.C. Sleppy: *J. Electrochem. Soc.*, 1961, vol. 108 (12), pp. 1097–1102.
2. M.P. Silva, D.E.J. Talbot: *Light Metals,* ed. P.G. Campbell, 118th Annual Meeting, TMS Light Metals Committee, Las Vegas, Nevada, 1989, pp. 1035-40.
3. S.A. Impey, D.J. Stephenson, and J.R. Nicholls: *Mater. Sci. Technol.*, 1988, vol. 4 (12), pp. 1126–32.
4. L.P.H. Jeurgens, W.G. Sloof, F.D. Tichelaar, and E.J. Mittemeijer: *Thin Solid Films*, 2002, vol. 418 (2), pp. 89–101.
5. J. Campbell: *Castings*, 1st ed., Butterworth-Heinemann, Oxford, 2000, pp. 62–63.
6. C.E. Eckert: *Proceeding of 3rd International Conference on Molten Aluminium Processing,* Des Plaines, AFS, Florida, 1992, pp. 17–50.
7. R. Fuoco, E.R. Correa, M.A. de Bastos, and L.S. Escudero: *AFS Trans.*, 1999, vol. 107, pp. 287–94.
8. S. Makarov, D. Apelian, and R. Ludwig: *AFS Trans.*, 1999, vol. 107, pp. 727–35.
9. A. Finkelstein, A. Schaefer, O. Chikova, and K. Borodianskiy: *Materials*, 2017, vol. 10, pp. 786–94.
10. D.J. Parker, C. Broadbent, P. Fowles, M.R. Hawkesworth, and P. McNeil: *Nucl. Instrum. Methods Phys. Res. Sect. A*, 1993, vol. 326 (3), pp. 592–607.
11. J.P.K. Seville, A. Ingram, and D.J. Parker: *Trans. I. Chem. E*, 2005, vol. 83 (A7), pp. 788–93.
12. D.J. Parker, R.N. Forster, P. Fowles, and P.S. Takhar: *Nucl. Instrum. Methods Phys. Res. Sect. A*, 2002, vol. 477 (1–3), pp. 540–45.
13. S. Langford, C. Wiggins, D. Tenpenny, and A. Ruggles: *Nucl. Eng. Des.*, 2016, vol. 302B, pp. 81–89.
14. R.C. Sindall, D. Dapelo, T. Leadbeater, and J. Bridgeman: *Flow Meas. Instrum.*, 2017, vol. 54, pp. 250–64.
15. A. Buffler, K. Cole, T.W. Leadbeater, and M.R. Heerden: *Int. J. Mod. Phys. Conf. Ser.*, 2018, vol. 48, pp. 1860113–23.
16. C.R.K. Windows-Yule, J.P.K. Seville, A. Ingram, and D.J. Parker: *Annu. Rev. Chem. Biomol. Eng.*, 2020, vol. 11, pp. 1–7.
17. M. Eesa and M. Barigou: *Int. J. Multiph. Flow*, 2008, vol. 34 (11), pp. 997–1007.
18. L. Liu and M. Barigou: *Chem. Eng. Sci.*, 2013, vol. 101, pp. 837–50.
19. P. Pianko-Oprych, A.W. Nienow, and M. Barigou: *Chem. Eng. Sci.*, 2009, vol. 64, pp. 4955–68.
20. W.D. Griffiths, Y. Beshay, D.J. Parker, and X. Fan: *J. Mater. Sci.*, 2008, vol. 43 (21), pp. 6853–56.
21. W.D. Griffiths, D.J. Parker, X. Fan, and M. Hausard: *Mater. Sci. Technol.*, 2010, vol. 26 (5), pp. 528–33.
22. X. Fan, D.J. Parker, and M.D. Smith: *Nucl. Instrum. Methods Phys. Res. Sect. A*, 2006, vol. 562, pp. 345–50.
23. K.S.W. Sing: *Adv Colloid Interface Sci.*, 1998, vols. 76–77, pp. 3–11.
24. M. Rafiee: *Use of Positron Emission Particle Tracking (PEPT) for Studying Laminar Mixing in Static Mixers*, Ph.D. Thesis, University of Birmingham, 2013, pp. 80–32.
25. D.J. Burnard: *Positron Emission Particle tracking of inclusions in cast liquid metals*, Ph.D. Thesis, University of Birmingham, 2014, pp. 160–80.
26. Y. Beshay: *The Application Of Positron Emission Particle Tracking To Study Non-metallic Inclusions In Metal Castings*, Ph.D. Thesis, University of Birmingham, 2010, p. 40.
27. M. Vahtrus, M. Umalas, B. Polyakov, L. Dorogin, R. Saar, M. Tamme, K. Saal, R. Lõhmus, and S. Vlassov: *Mater. Charact.*, 2015, vol. 107, pp. 119–24.
28. E. W. Pitzer: *Activated alpha alumina, its formation, and its use:* Patent Application Serial No. 120,808 18 Claims. (CI. 260-683.3), United States Patent Office, 1949.
29. L. Samain, A. Jaworski, M. Edén, D.M. Ladd, D.K. Seo, F.J.G. Garcia, and U. Häussermann: *J. Solid State Chem.*, 2014, vol. 217, pp. 1–8.
30. S. Chakraborty, T. Das, S. Banerjee, S. Subramanian, H.D. Sarma, and M. Venkatesh: *Nucl. Med. Biol.*, 2006, vol. 33 (4), pp. 585–91.